LHC-Project-Report-1181

Proton-Nucleus Collisions at the LHC: Scientific Opportunities and Requirements

Editor: *C. A. Salgado*[1]

Authors: *J. Alvarez-Muñiz*[1], *F. Arleo*[2], *N. Armesto*[1], *M. Botje*[3], *M. Cacciari*[4], *J. Campbell*[5], *C. Carli*[6], *B. Cole*[7], *D. D'Enterria*[8,9], *F. Gelis*[10], *V. Guzey*[11], *K. Hencken*[12,*] *P. Jacobs*[13], *J. M. Jowett*[6], *S. R. Klein*[13], *F. Maltoni*[14], *A. Morsch*[8], *K. Piotrzkowski*[14], *J. W. Qiu*[15], *T. Satogata*[15], *F. Sikler*[16], *M. Strikman*[17], *H. Takai*[15], *R. Vogt*[13,18], *J. P. Wessels*[8,19], *S. N. White*[15], *U. A. Wiedemann*[20], *B. Wyslouch*[21,†] *M. Zhalov*[22]

[1] Departamento de Física de Partículas and IGFAE, U. Santiago de Compostela, Galicia, Spain
[2] LAPTH, Universitè de Savoie et CNRS, Annecy-le-Vieux Cedex, France
[3] NIKHEF, Amsterdam, The Netherlands
[4] LPTHE, Université Pierre et Marie Curié (Paris 6), France
[5] Theoretical Physics Department, Fermilab, Batavia, IL, USA
[6] Beams Department, CERN, Geneva, Switzerland
[7] Nevis Laboratories, Columbia University, New York, NY, USA
[8] Physics Department, Experimental Division, CERN, Geneva, Switzerland
[9] ICREA, ICC-UB, Univ. de Barcelona, 08028 Barcelona, Catalonia
[10] IPTh, CEA/DSM/Saclay, 91191, Gif-sur-Yvette Cedex, France
[11] Jefferson Lab, Newport News, VA, USA
[12] Institut für Physik, Universität Basel, Switzerland
[13] Nuclear Science Division, Lawrence Berkeley National Laboratory, Berkeley, CA, USA
[14] Université Catholique de Louvain, Louvain-la-Neuve, Belgium
[15] Physics Department, Brookhaven National Laboratory, Upton, NY 11973, USA
[16] KFKI Research Institute for Particle and Nuclear Physics, Budapest, Hungary
[17] Department of Physics, Pennsylvania State University, USA
[18] Physics Department, University of California at Davis, Davis, CA, USA
[19] Institut für Kernphysik, Universität Muenster, D-48149 Muenster, Germany
[20] Physics Department, Theory Division, CERN, Geneva, Switzerland
[21] LLR Ecole Polytechnique, 91128 Palaisseau Cedex, France
[22] St. Petersburg Nuclear Physics Institute, Gatchina, Russia

Abstract

Proton-nucleus (p+A) collisions have long been recognized as a crucial component of the physics programme with nuclear beams at high energies, in particular for their reference role to interpret and understand nucleus-nucleus data as well as for their potential to elucidate the partonic structure of matter at low parton fractional momenta (small-x). Here, we summarize the main motivations that make a proton-nucleus run a decisive ingredient for a successful heavy-ion programme at the Large Hadron Collider (LHC) and we present unique scientific opportunities arising from these collisions. We also review the status of ongoing discussions about operation plans for the p+A mode at the LHC.

[*] Current address: ABB Switzerland Ltd., Corporate Research, Baden-Dättwil, Switzerland
[†] On leave of absence, Massachusetts Institute of Technology, Cambridge, MA 02139, USA

Contents

1. EXECUTIVE SUMMARY

Heavy-ion physics is an integral part of the baseline experimental programme of the CERN Large Hadron Collider (LHC). After normal operations have been established, the LHC is running for about 8 months per year with proton beams and for one month per year with nuclear beams. Three of the four experiments (ALICE, ATLAS and CMS) participate in the LHC nuclear beam programme[1]. So far, only collisions with Pb nuclei are firmly scheduled, while operational plans for proton-nucleus (p+A) collisions are still preliminary. However, the LHC is a versatile hadron collider that allows, in principle, the collision of asymmetric (A+B) nuclear beams. All three LHC experiments have included p+A collisions in their physics performance studies and have discussed their importance.

The proton-nucleus programme serves a dual purpose. It provides, on the one hand, baseline measurements for the nucleus-nucleus program. Experience from previous heavy ion programs (CERN SPS, RHIC) shows that a p+A baseline is essential for the interpretation of some of the main discoveries (e.g. J/ψ-suppression, jet quenching, ...). This document identifies an analogous need for p+A collisions at the LHC. A p+A programme also offers unique possibilities for specific investigations in various domains of Quantum Chromodynamics (QCD).

This document presents an updated description of: i) the accelerator issues for collision of asymmetric systems at the LHC; ii) the uncertainties in nuclear parton distribution functions and benchmark cross section for hard processes; iii) the new opportunities made available to study parton saturation, ultra-peripheral collisions and measurements, which are of interest to astrophysics; and iv) the experimental issues related to the special conditions of the p+A run.

The main conclusions of this document are the following:

- Preliminary considerations indicate the feasibility to run the LHC in p+A mode without major modifications of the machine. We consider here a canonical situation in which the energy of the p+Pb run ($\sqrt{s} = 8.8$ TeV) corresponds to the charge-over-mass ratio scaling with respect to the proton top LHC energy. The estimated luminosity is $L = 10^{29}$cm^{-2}s^{-1} for p+Pb collisions. Asymmetric collisions imply also rapidity shifts with respect to the A+A and p+p systems. This effect can be reduced by colliding deuterons with nuclei instead of protons. The realisation of the d+A mode, however, needs significant hardware modifications of the injector chain.

- The knowledge of nuclear parton distributions is deficient for the kinematics accessible at the LHC. This has negative consequences for the interpretation of the A+A data and a p+A run is indispensable for benchmarking: For most of the duration of the LHC programme, a p+A run will be the only experimental possibility to reduce systematic uncertainties arising from yet unmeasured parton distributions. In this document we study possible constraints from different processes. Assuming a running time of 10^6 s the corresponding integrated luminosity of 0.1 pb^{-1} will make the measurements considered in this document feasible. A significantly smaller integrated luminosity will compromise the performance for several observables. On the contrary, an increase in luminosity by a factor of 10 will be beneficial for observables with the smallest cross sections, especially those involving high-p_T photons and heavy bosons.

- p+A collisions at the LHC offer unique possibilities for the study of small-x physics with

---

[1]Although LHCb has not so far considered running with nuclear beams, there is in principle no technical difficulty preventing this experiment from doing so. Their excellent detection capabilities at forward rapidities would be very useful for proton-nucleus measurements.

nuclear targets, extending the kinematically accessible regime by several orders of magnitude in x and Q^2 from those presently available. This provides an excellent opportunity for the study of the saturation of partonic densities. Other physics opportunities include ultra-peripheral (electromagnetic) collisions and measurements of cross sections of interest for cosmic ray physics.

- The LHC experiments have proven capabilities to exploit the physics opportunities of a p+A run at the quoted luminosity. For some observables, running p+Pb at the same nucleon-nucleon centre-of-mass energy as Pb+Pb would have the advantage of reducing systematic uncertainties for benchmark perturbative processes. Further reduction of the uncertainties, for the case of rapidity asymmetric detectors, necessitates operation of both p+A and A+p modes. For nuclear PDF and small-x studies, the largest possible energy is preferred. This document provides important arguments for the timely scheduling of p+A runs.

2. INTRODUCTION

With the LHC, high-energy nuclear collisions have reached the TeV scale for the first time. This has opened up a discovery regime, which is currently being vigorously explored exploiting the first long run with Pb+Pb collisions at $\sqrt{s_{NN}}$= 2.76 TeV. The corresponding first results on multiplicities, elliptic flow, jet quenching and other observables have been published [1, 2, 3, 4, 5]. The top LHC energy of $\sqrt{s_{NN}}$=5.5 TeV exceeds that of the Relativistic Heavy Ion Collider (RHIC) by almost a factor of 30. The increase in centre-of-mass energy will be even larger for p+Pb collisions ($\sqrt{s_{NN}}$=8.8 TeV). This large jump in energy translates into a kinematical reach in Bjorken-x and virtuality Q^2 that is several orders of magnitude beyond that achieved in all other previous experiments with nuclear collisions.

Based on the current understanding of nucleus-nucleus collisions, there are in particular two classes of questions where the extended kinematic reach of the LHC is expected to give access to qualitatively new phenomena. i) Hard probes are produced at unprecedented rate at the LHC. The established strong sensitivity of these hard probes provides a promising and diverse method for a detailed characterization of the properties of the produced dense QCD matter; ii) Much smaller momentum fractions x become relevant for particle production. On the one hand, the large parton densities at small-x are expected to make the system initially produced in the collision denser, hotter and thus longer lived. As a result, a characterization of parton distributions at small-x is important for the understanding of the initial conditions from which dense QCD matter emerges — as also demonstrated by the first particle multiplicity data [1] showing striking scaling features with respect to the smaller energy (RHIC) data. On the other hand, the dense initial partonic system is of interest in its own, since one expects to access with increasing $\sqrt{s}$ a novel high density regime of QCD in which parton distributions are saturated up to perturbatively large virtualities. As discussed in this document, measurements of proton-nucleus collisions are crucial for exploiting the opportunities of these two classes of measurements at the LHC.

Normalization runs with proton-nucleus (p+A) collisions have long been recognized as a crucial component of the LHC heavy-ion program. More generally, this is because the characterization of signatures of the QCD matter created in heavy ion collisions relies on benchmark processes with elementary collision partners, in which final-state medium effects such as collective phenomena are largely absent. To some extent, such benchmarking can be done with data from proton-proton collisions which characterize production processes in the absence of both initial and final state medium effects. However, to disentangle the initial state effects from those final state effects which characterize the properties of the produced dense QCD matter, proton-nucleus collisions are crucial. The absence of strong final state medium effects in proton-nucleus collisions provides a unique opportunity for characterizing the nuclear dependence of parton distribution functions at a hadron collider. This benchmarking of the initial conditions is of particular importance for heavy-ion collisions at the LHC, since e+A DIS data will not be available any time soon for a large range of the kinematically relevant small-x values. Beyond benchmarking, proton-nucleus collisions are also expected to provide access to qualitatively new features of the small-x structure of matter.

Since the last extensive discussions of proton-nucleus collisions at the LHC [6, 7, 8, 9], significant experimental and theoretical developments have occurred in this area. In particular, the technical challenge of running a hadron collider in an asymmetric mode has been mastered at RHIC, where deuterium-gold measurements have provided the decisive benchmark experiments for discoveries in the corresponding nucleus-nucleus program. The extrapolation of these

results allow us now to substantiate statements about the required luminosity and experimental coverage for a successful proton-nucleus normalization run at the LHC. Further, recent theoretical developments in studying the energy evolution of Quantum Chromodynamics at high parton densities and small-x have added significantly to the physics case for a proton-nucleus run at the LHC. In fact, a growing physics community has started to work towards a dedicated electron-nucleus collider for elucidating the small-x structure of matter [10, 11]. The question arises to what extent proton-nucleus runs at the LHC can help to prepare and complement such a future large scale project.

The purpose of this document is to provide a brief update of our current understanding of how the LHC could operate in p+A mode, how a proton-nucleus run could be exploited to optimally support a successful heavy-ion programme at the LHC, and which additional scientific opportunities arise from proton-nucleus collisions at the LHC.

3. THE LHC AS A PROTON-NUCLEUS COLLIDER

Although proton-nucleus collisions (p+A) at the LHC had been discussed in the physics community for some years, they were not formally included in the initial "baseline" LHC machine design [12], which included only symmetric p+p and Pb+Pb collisions. The p+A mode of operations (as well as collisions between lighter ions) was considered as an option, to be studied and implemented later. The rationale for this at the time was twofold:

- The need to focus available resources on what was needed for the startup of the LHC.
- The baseline modes of operation are the most difficult in many respects.

With the LHC starting to explore the p+p and Pb+Pb physics programmes, a need to investigate the feasibility of the p+A mode of operation of the LHC appears. Meanwhile some concerns have emerged from the experience gained at RHIC. In this document we have tried to respond to these concerns with a preliminary study of the feasibility and potential performance.

3.1 RHIC Experience

RHIC operated with deuteron-gold collisions (d+Au) in 2003 and 2008 [13, 14]. The 2003 run was the first for an asymmetric hadron collider, and faced several challenges. Some relevant to the LHC proton-ion programme include multi-species injector performance, setup time constraints, injection with equal rigidity vs. equal revolution frequency between the two beams, and collision geometries of dissimilar species. At RHIC a proton-gold run was considered but required either large deviations in the arcs or movement of the common DX magnets. So, the option of a more symmetric charge-over-mass ratio as in a d+Au colliding system was adopted.

Careful attention should be given to dual-species injector performance and reliability, particularly since any bottleneck will significantly impact the performance of short LHC p+Pb runs. Injector emittance and intensity development ultimately limited RHIC performance during the 2003 d+Au run. Later improvements in injector Au performance for dedicated Au+Au operations provided the basis for the 2008 d+Au run, which delivered six times the integrated luminosity of that in 2003.

RHIC d+Au took 18 days of development to first collisions, and an additional 20 days to the start of physics development. This time included the development of new acceleration/β-squeeze ramps (see below) and about 6 days of detector setup operations. The LHC p+Pb setup will likely be shorter since LHC p+p and Pb+Pb will precede p+Pb operations.

Early in the RHIC 2003 d+Au run, injection and ramping setup were changed from the same magnetic rigidity in both rings to the same RF frequency in both rings—this was necessary to avoid beam-beam modulation and serious beam losses (up to 50 % of stored beam) during injection and ramping, even with interaction region beam separations of 10 sigma. For the LHC, beam-beam compensation and transverse dampers should be investigated, perhaps with modifications, to control emittance growth and beam loss from this mechanism.

The collision geometry of the LHC for p+Pb should be studied for asymmetries, in conjunction with the LHC experiments. The RHIC d+Au run required swaps of power supply shunts on DX dual-ring magnets to satisfy the orbit geometry requirements of different Z/A species in each ring. This created a $1\,\mu\mathrm{rad}$ collision angle within the experiments, marginally affecting detector acceptances.

3.2 Injector chain for proton-ion or deuteron ion operation of the LHC

For the reasons given above, only preliminary considerations on LHC filling for p+A or d+A operation have been made. The injector chains for protons and ions are distinct at the low energy end, i.e., the initial Linac and the first synchrotron. Clearly, as much as possible of the existing LHC injector chains must be used to allow proton (deuteron)-ion operation of the LHC at a reasonable cost.

We assume that one of the two LHC rings will be filled with ions featuring the nominal bunch pattern for ion-ion operation. Furthermore, we assume that the second LHC ring must be filled with protons or deuterons in the *same nominal ion* bunch pattern. The "lazy" solution, to fill the other ring with the usual p+p bunch pattern and to have at least some encounters at the interaction points (but some ion bunches may never collide with a proton bunch), would have many disadvantages and is not envisaged.

3.21 Injector chain for proton-ion operation

Assuming that one LHC ring is filled with a nominal Pb-ion beam (bunch population, emittances, filling pattern) and that the proton bunches have the same geometric beam sizes and bunch pattern, an intensity of the order of 10^{10} protons per bunch is needed to reach the required luminosity of the order of $10^{29}\mathrm{cm}^{-2}\mathrm{s}^{-1}$.

The LHC ion ring will be filled using the standard ion injector chain in the standard way (yielding the nominal LHC ion bunch pattern). The problem consists in finding a scheme that allows the LHC proton ring to be filled with protons in the same bunch pattern as the ions. Two distinct schemes have been identified (although many more probably exist). Each of them uses the LHC proton injector chain but applies longitudinal gymnastics that are very different from nominal proton filling.

- The first scheme is based on the experience with generation of LHC (proton) pilot bunches in the PS Booster. Every Booster ring provides one bunch per cycle and each of these bunches corresponds to one LHC bunch (no bunch splitting along the rest of the chain). These bunches are injected into adjacent PS buckets. The harmonic number of the PS ($h = 16$ may be a good choice) is chosen so that the bunch spacing is sufficient for the PSB recombination line kicker. The PS harmonic number must be increased gradually to $h = 21$ to obtain the right 100 ns bunch spacing and the 40 MHz and 80 MHz RF systems must be used to shorten the bunches before ejection towards the SPS. The four bunches provided per PS proton cycle correspond to the four ion bunches per PS ion cycle. The

rest of the LHC injector chain is very similar (accumulation of up to 13 injections on an SPS low energy plateau, acceleration and transfer to the LHC) for proton and ion filling and even slightly simpler (no stripping in the transfer line between PS and SPS and, thus, a higher magnetic field in the SPS, no "fixed" frequency non-integer harmonic acceleration needed for protons).

- The second scheme aims at faster filling of the LHC proton ring. Every bunch provided by the PS Booster corresponds to one LEIR/PS ion cycle and, thus, has to provide four LHC proton bunches. This scheme requires more elaborate longitudinal gymnastics than the first one (but they are still simpler than the gymnastics applied routinely in operations to provide, e.g., the beam for LHC p+p operation).

At a first glance, the proton beam needed for ion-proton operation of the LHC can be provided by the injector chain at a reasonable cost and without major hardware upgrades.

3.22 Injector Chain for Deuteron-Ion Operation of the LHC

Schemes for filling one LHC ring with deuterons have been given only very preliminary consideration. In principle, one could imagine one of the following two scenarios:

Deuterons via the ion injector chain (Linac 3 and LEIR): In order to provide both ions and deuterons via the ion injector chain, sufficiently fast switching between these two species at the low energy part of Linac3 would be required. Furthermore the radio-frequency quadrupole (RFQ) used for ions would not perform well for deuterons. Thus, a dedicated deuteron RFQ, adjusted to higher input particle velocity and voltage for extraction from the source, would be necessary. In summary it is clear that a dedicated deuteron source and RFQ and a switchyard allowing switching between ions and deuterons is the minimum requirement.

Deuterons via the proton injector chain (Linac 2 PSB): Linac4 will replace the present Linac2 as PS Booster injector from 2015 on, so this option will not be available after that time. The PS Booster will then be converted for H^- charge exchange injection so deuterons for the LHC would have to be produced from D^- injection. Whereas the simple drift tube structure of Linac2 could, in principle, accelerate D^- (with a velocity half that of protons), this is not the case for Linac4 which consists of three different accelerating structures. A dedicated D^- source and RFQ would be needed in any case and represents a significant investment.

Using Linac2 for D^- acceleration would have limited impact on proton beams for other facilities.

These very preliminary investigations lead to the conclusion that the injector chain cannot be upgraded for LHC deuteron-ion operation without major hardware upgrades and investments (in equipment and manpower). Further detailed investigations are needed to confirm whether either of the schemes outlined above is feasible. In any case, deuterons in the LHC will require several years' lead time.

3.3 LHC Main Rings

The LHC differs from RHIC in its two-in-one magnet design, a single magnet ring with two beam apertures, rather than the two rings of independent magnets of the Brookhaven machine. With asymmetric beams in the machine this difference is crucial and determines many key beam parameters and experimental conditions.

	p+p	Pb+Pb	p+Pb	d+Pb
$E_{\mathrm{N}}/\mathrm{TeV}$	7	2.76	(7,2.76)	(3.5,2.76)
$\sqrt{s_{\mathrm{NN}}}/\mathrm{TeV}$	14	5.52	8.79	6.22
Δy	0	0	0.46	0.12

Table 1: Beam energy per nucleon, $E_{\mathrm{N}} \approx (p_{\mathrm{proton}}, p_{\mathrm{Pb}})c/A$, center-of-mass collision energy per nucleon, $\sqrt{s_{\mathrm{NN}}}$, and central rapidity shift, Δy, of colliding nucleon pairs for maximum rigidity colliding beams in the LHC; Δy is in the direction of the lighter ion.

For definiteness, we consider the case of protons colliding with lead ions; the case with other beams is analogous. The LHC accelerates protons through the momentum range

$$0.45\,\mathrm{TeV}\ \text{(injection from SPS)}\ \leq p_{\mathrm{proton}} \leq 7\,\mathrm{TeV}\ \text{(collision)}. \tag{1}$$

Since the magnetic field is equal in the two apertures, there is a relation (equal magnetic rigidity) between the momenta of proton and lead ion:

$$p_{\mathrm{Pb}} = Q\,p_{\mathrm{proton}}, \tag{2}$$

where $Q = Z = 82$ and $A = 208$ for fully stripped Pb ions.

While this places many constraints on p+Pb operation, it does, on the other hand, simplify some aspects: the geometry of the beam orbits does not change at all so there are no complications with separation magnets (c.f., the movement of "DX" magnets to adjust the collision geometry in RHIC).

The centre-of-mass energy and central rapidity shift for colliding nucleon pairs within ions (Z_1, A_1), and (Z_2, A_2)

$$\sqrt{s_{\mathrm{NN}}} \approx 2c\,p_{\mathrm{proton}}\sqrt{\frac{Z_1 Z_2}{A_1 A_2}}, \qquad \Delta y \approx \frac{1}{2}\log\frac{Z_1 A_2}{A_1 Z_2} \tag{3}$$

are direct consequences of the two-in-one magnet design via (2); see also Table 1.

Because of (2), the two beams have different speeds and revolution periods on nominal orbits of the same length. The RF systems of the two rings of the LHC are perfectly capable of operating independently at the different frequencies required during injection and ramping. However they must be locked together at identical frequencies in physics conditions to keep the collision points between bunches from moving. This forces the beams onto distorted, off-momentum orbits of different lengths but identical revolution periods. The amplitude of the distortion remains within the limits considered acceptable for the LHC only for $p_{\mathrm{proton}} > 2.7\,\mathrm{TeV}/c$. This imposes a lower bound on possible collision energies.

At lower energies, therefore, the beams necessarily have different revolution periods. Each Pb ion bunch encounters up to 5 or 6 proton bunches as it traverses one of the straight sections around the LHC experiments where the two beams circulate in a common beam pipe. At injection energy, these encounter points move along the straight section (in the direction of the proton beam) at a rate of 0.15 m per turn. They then disappear into the arcs only to re-emerge a few seconds later in the next experimental straight section. As the main bend field is ramped up, this motion slows down, finally freezing when the energy is high enough that the RF frequencies can be locked together. A re-phasing operation (known as "cogging") to peg

the collision points in their proper places may still need to be carried out (although it may be possible to arrange the timing so that this takes place in the last part of the ramp).

During injection and ramping the bunches are separated in all the common sections of the LHC so that they never collide head-on but nevertheless have some long-range beam-beam interaction. It was shown [15] that the separation is sufficient that the magnitudes of these interactions, expressed either as kicks or parasitic beam-beam tune-shifts, are very small. The strength of the corresponding "overlap knock-out" resonances [16] is also relatively small. For these reasons, it appears unlikely that the moving beam-beam encounters will have the severe consequences experienced in analogous conditions at RHIC (see above) and, earlier still, at the ISR [16]. However this is a tentative conclusion requiring more detailed justification.

Moreover, the LHC, unlike RHIC, will have the benefit of four independent transverse feedback systems, one per plane and per ring, with bandwidth high enough to act on individual bunches. This promises to be a powerful tool in damping any coherent motion induced by the moving encounters.

The moving encounters might also affect the operation of those beam position monitors that see both beams. Some modifications of their electronics may be necessary in order to implement appropriate signal gating.

With the fairly conservative assumptions of bunches of 7×10^7 Pb ions (nominal intensity for the Pb+Pb mode) colliding with bunches of 1.15×10^{10} protons (10% of the nominal p+p mode intensity), with the usual beam emittances, optics and bunch train structure for Pb beams, a typical initial peak luminosity would be

$$ L \approx 1.5 \times 10^{29} \text{cm}^{-2} \text{s}^{-1}. \tag{4} $$

Performance beyond this level might be attainable with, most likely, higher proton bunch intensity. However it should be remembered that p+Pb runs at the LHC are likely to be rather short, with limited time available to maximise performance. On the other hand, by the time a p+Pb run is scheduled, operational procedures ought to be well-established and smooth. More concrete luminosity projections will come from deeper studies and, most importantly, initial experience of running the LHC with proton and nuclear beams.

For a given luminosity, this choice of the maximum possible number of bunches is more likely to generate some cancellation among multiple, weaker, moving parasitic encounters. However alternative sets of parameters (e.g., half the number of nominal intensity Pb bunches against the same number of 2.3×10^{10} proton bunches), would lead to similar luminosity. These could be of interest if the total Pb intensity is limited because of collimation inefficiency (e.g., before the proposed dispersion suppressor collimators are installed in the collimation insertions).

The question of switching the directions of the p and Pb beams has been raised. This is perfectly feasible. Clearly the experimental advantages would have to be weighed against the set-up time (presently hard to estimate) during a short p+A run. If only one direction is possible, it appears that all experiments would prefer—or accept—protons in Ring 1 and Pb ions in Ring 2.

In conclusion, preliminary studies since have found no major obstacles, in terms of hardware modifications or beam dynamical effects, to colliding protons and lead nuclei in the LHC with adequate luminosity. However further studies of the beam dynamics are essential to demonstrate the feasibility of what will probably be the most complicated mode of operation of the LHC.

4. p+A AS A BENCHMARK FOR A+A

Historically, the benchmark role of p+A (or d+Au at RHIC) collisions has been essential for the interpretation of the heavy-ion results. At RHIC, two main examples arise: i) the absence of suppression in the transverse momentum spectrum of the inclusive hadron production [17, 18] proved the jet quenching hypothesis as the genuine final-state effect at work to explain the observed deficit of high-p_T hadrons in Au+Au collisions [19, 20]; ii) the moderate suppression of the J/ψ at central rapidities [21] contrasts with the stronger suppression predicted by models extrapolating from SPS data, affecting the interpretation of the corresponding hot nuclear matter effects in Au+Au . At the CERN SPS, the experimental data on several p+A systems at different energies are fundamental for the interpretation of the results on J/ψ suppression in Pb+Pb collisions [22].

The nuclear modifications of the production cross sections for hard processes in p+A compared to p+p collisions are studied here with special emphasis on those involving large virtualities. Predictions for cross sections with different degrees of nuclear effects are collected. These processes are expected to provide key measurements of the validity of QCD factorization in nuclear collisions as well as constraints on the nuclear parton distribution functions.

The QCD factorization theorem [23] provides a prescription for separating long-distance and short-distance effects in hadronic cross sections. The leading power contribution to a general hadronic cross section involves only one hard collision between two partons from the incoming hadrons with momenta p_A and p_B. The cross section can be factorized as [23]

$$
E_h \frac{d\sigma_{AB \to h(p')}}{d^3 p'} = \sum_{ijk} \int dx' f_{j/B}(x') \int dx\, f_{i/A}(x) \int dz\, D_{h/k}(z)\, E_h \frac{d\hat{\sigma}_{ij \to k}}{d^3 p'}(xp_A, x'p_B, \frac{p'}{z}),
$$
(5)

where $\sum_{ijk}$ runs over all parton species and all scale dependence is implicit. The $f_{i/A}$ are twist-2 distributions of parton type i in hadron A (parton distribution functions, PDFs) and the $D_{h/k}$ are fragmentation functions for a parton of type k to produce a hadron h.

In the nuclear case, the incoherence of the hard collisions implies that the nuclear PDFs (nPDFs) contain a geometric factor, so that the hard cross sections are proportional to the overlap between the two nuclei. The degree of overlap can be estimated experimentally in a probabilistic approach proposed by Glauber [24]. This fixes the baseline, i.e. the "equivalent number of p+p collisions", N_{coll}, to which the central A+A cross section measurements are compared, to quantify the effects on such observables of the hot and dense matter. The Glauber model is, however, not a first-principles calculation and experimental checks of this model are of utmost importance for the interpretation of the main results expected in the A+A runs.

4.1 Nuclear parton distribution functions

Equation (5) reveals the need for a precise knowledge of the PDFs for the LHC physics programme. For the proton case, the PDFs are constrained by a large number of data — especially from HERA and the Tevatron — in global fits performed at LO, NLO or NNLO. In the nuclear case, much less extensive experimental data on nuclear DIS are available in the perturbative region ($Q^2 \gtrsim 1$ GeV^2), only for $x \gtrsim 0.01$. As a result, there are large uncertainties in the nPDFs relevant for LHC kinematics. The most recent versions of the nPDFs global fits at NLO are EPS09 [25], HKN07 [26] and nDS [27] — also Schienbein *et al.* [28] performed a similar global fit but did not release a set for public use yet. Studies of the uncertainties following the Hessian method are available [25, 26] and also released for public use. All sets of nPDFs fit

data on charged leptons DIS with nuclear targets and Drell-Yan in proton-nucleus collisions. Checks of the compatibility with other hard processes are also available: the inclusive particle production at high transverse momentum from d+Au collisions at RHIC has been included in the analysis of [25] without signs of tension among the different data sets; the compatibility with neutrino DIS data with nuclear targets has also been checked in Ref. [29][2]. Moreover, the most recent data from Z-production at the LHC [30] also show good agreement with the factorization assumption although errors are still moderately large. In spite of these successes, the gluon distribution remains poorly constrained for the nucleus, as can be seen in Fig. 1 where different sets of nPDFs are shown, together with the corresponding uncertainty bands. DGLAP evolution is, however, very efficient in removing the nuclear effects for gluons at small-x, which quickly disappear for increasing Q^2. In this way, these uncertainties become smaller for the hardest available probes — see Fig. 1 — except for the large-x region where substantial effects could survive for large virtualities. This region is, however, dominated by valence quarks which in turn are rather well constrained by DIS data with nuclei.

An alternative approach [31] computing the small-x shadowing by its connection to the hard diffraction in electron-nucleon scattering has been used to obtain the nuclear PDF at an initial scale Q_0 which are then evolved by NLO DGLAP equations. The inputs in this calculation are the diffractive PDFs measured in DIS with protons at HERA. These distributions are dominated by gluons, resulting in a stronger shadowing for gluons than the corresponding one for quarks. In Fig. 1 the results from this approach for the gluon case are also plotted. The differences at small-x become even larger at smaller virtualities (not shown) [31].
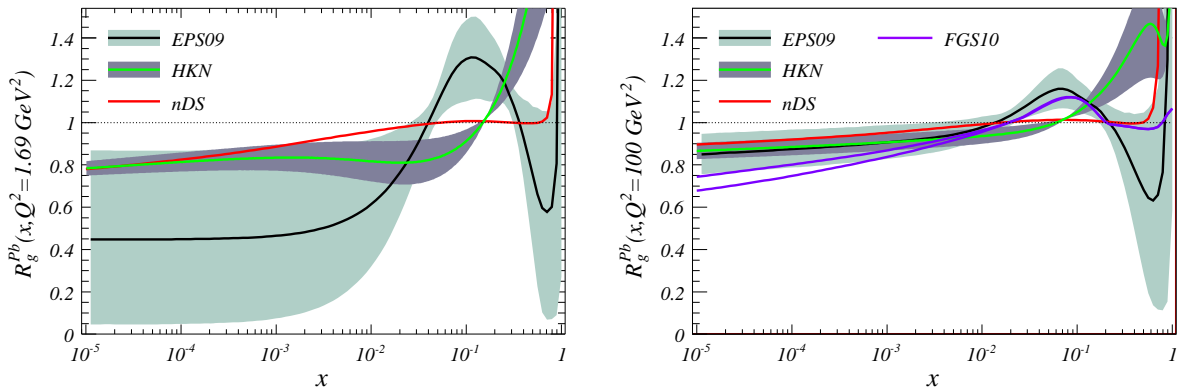

Fig. 1: Current knowledge of nuclear PDFs, shown as the ratio of bound over free proton gluon distributions, $R_g^{Pb}(x, Q^2)$, obtained by the NLO global fits EPS09 [25], HKN07 [26] and nDS [27] at two different virtualities, $Q^2 = 1.69$ GeV^2 and Q^2=100 GeV^2. Also shown for $Q^2 = 100$ GeV^2 are the results from Ref. [31] (FGS10) in which gluon shadowing is computed from the DIS diffraction cross section measured at HERA.

It is worth noticing that in contrast to RHIC, where there are constraints at mid-rapidity $(x \gtrsim 10^{-2})$ for nuclear distributions from DIS and DY data, the LHC will probe completely unexplored regions of phase space. This complicates the interpretation of the A+A data before a p+A benchmarking programme removes these uncertainties, e.g. for the suppression of high transverse momentum particles observed in [3]. The experimental data from d+Au collisions at RHIC have already proven to be an appropriate testing ground for nPDFs studies: as mentioned before, data on inclusive production at high-p_T has been included in global fits, providing constraints for gluons; nPDFs are also extensively used in phenomenological studies of hard probes

---

[2]See, however, Ref. [28] for contradicting results.

at RHIC. On the other hand, the strong suppression found in forward rapidity hadron data [32] has challenged the interpretation in terms of a modification of PDFs alone. Indeed, a global fit including these data is possible [33] but resulting in a sizable tension with DIS data. The presence of final-state effects and/or the inadequacy of the collinear factorization formalism — and the corresponding onset of saturation of partonic densities — are two possible explanations for new mechanisms at work in this rapidity range.

Reducing the uncertainties on the initial structure of the colliding nuclei is extremely important also for central conceptual insights expected from the LHC, such as the evolution of the system in A+A collisions from cold nuclear matter to hot partonic matter. For all dynamical models of this evolution, knowledge of the initially-produced particle density is crucial. Ultimately, however, this density varies with the uncertainty of the nPDFs and controlling these uncertainties is a decisive step in addressing one of the central issues in the dynamics of heavy-ion collisions.

In summary, no other experimental conditions, except p+A collisions at the LHC, exist or will exist in due time to pin down the parton structure of the nucleus in the necessary kinematic regime for the A+A studies.

4.2 Processes of interest for benchmarking

The characterization of the medium properties in heavy-ion collisions is performed through processes which couple to the medium in a theoretically well-controlled manner. Among these processes, the hard probes — e.g. jets, heavy flavor, or quarkonia — require good knowledge of the nPDFs and other cold nuclear matter effects. Soft probes such as collective flow do not require, in principle, any benchmark as the corresponding signals have so far not been observed in more elementary collisions — although some recent results from CMS p+p collisions [34] admit an interpretation in terms of collective phenomena. Other hard processes, which do not involve the strong interaction in the final state, such as direct photon production or W/Z production, may also serve as benchmarks and as checks of the factorization hypothesis, Eq. (5). In this section we review the uncertainties associated with hard processes due to nPDFs. We select processes involving large virtualities, where the nuclear effects in the parton densities are expected to be small, and processes involving smaller virtualities where the effects are larger.

4.21 Jets

The modification of the spectrum of particles produced at large transverse momentum, *jet quenching*, is one of the main probes for the properties of the hot and dense matter formed in heavy ion collisions at RHIC. Some of the most interesting results from the first year LHC run refer to this observable [3, 4, 5]. For this reason, studies of (multi)jet production in p+A collisions are of great importance as a "cold QCD matter" benchmark. Jet rates in minimum bias p+Pb collisions at the LHC (2.75+7 TeV per nucleon) have been computed at NLO using the Monte Carlo code in [35, 36, 37], with a renormalization/factorization scale $\mu = E_T/2$ where E_T is the total transverse energy in the event, and using the CTEQ6.1M [38] nucleon parton densities. Implementing a fixed-order computation, this code produces at most 3 jets and contains no parton cascade. The precision of the computation, limited by CPU time, and the uncertainties due to the choice of nucleon and nuclear parton densities, isospin corrections, scale fixing,..., together with the influence of the jet finding algorithm and the possibilities to explore different nuclei and collision energies, have been discussed elsewhere [6, 7].

Figure 2 shows the results for 1-, 2- and 3-jet yields within two central, one backward and one forward pseudorapidity windows in the LHC frame (asymmetric for these beam momenta), as a function of the E_T of the hardest jet within the acceptance. The yields, computed here for a luminosity $\mathcal{L} = 10^{29}$ cm^{-2}s^{-1} integrated in one month (10^6 s) run, are quite large — for simplicity, the corresponding scale can be read in the two right panels of Fig. 2. For example, in the backward region, $-4.75 < \eta < -3$, yields above 10^5 1-jet events per GeV can be achieved for $E_{Thardest} < 80$ GeV. In the same region, the yields of events with 2 jets within the acceptance are not reduced by than a factor 100. Thus, studies of cold nuclear matter effects on multi-jet production should be feasible.

The effect of nuclear corrections to PDFs is very small [$\mathcal{O}$(20%) at most] and hardly visible in the yields in Fig. 2. The corresponding hot nuclear matter effects in Pb+Pb are expected to be much larger. The energy interpolation to make the ratios with the expectations from p+p without nuclear effects should be safe enough for the required degree of accuracy.
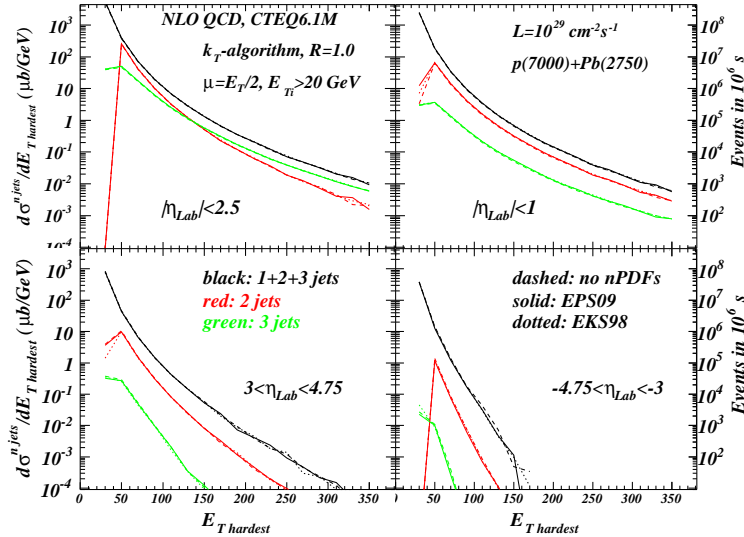

Fig. 2: 1-, 2- and 3-jet cross section as a function of the E_T of the hardest jet within the acceptance. Different pseudorapidity windows (in the laboratory frame) computed for minimum bias p+Pb collisions at the LHC (2.75+7 TeV per nucleon) are considered. Dashed lines are the results without nuclear modification to the PDFs; solid lines are the results with EPS09 [25]; dotted lines are results with EKS98 nuclear corrections [39, 40] to nucleon parton densities. Also shown is the scale for corresponding yields for a luminosity $\mathcal{L} = 10^{29}$ cm^{-2}s^{-1} in one month of running.

4.22 Processes involving electroweak bosons

The production of electroweak bosons has not been studied in nuclear collisions before the LHC due to the limitations in energy. However, already during the first lead-lead run, Z production has been reported by ATLAS [30] and CMS [41]. At leading order, the main mechanism of W/Z production is the quark-antiquark channel and the fact that valence quark distributions are rather well constrained by nuclear DIS at large-x makes this probe a good one for constraining the sea quark distributions [42, 43]. In fact, the asymmetrical nature of p+A collisions provide an excellent opportunity for nuclear PDF studies [43].

On the other hand, the increasing relevance of jet physics in heavy-ion collisions render Z+jet measurements of great importance to improve the jet energy calibration. The inclusive Z+1jet cross section is known at next-to-leading order in the strong coupling both for light and heavy-quark jets [44, 45, 46, 47].
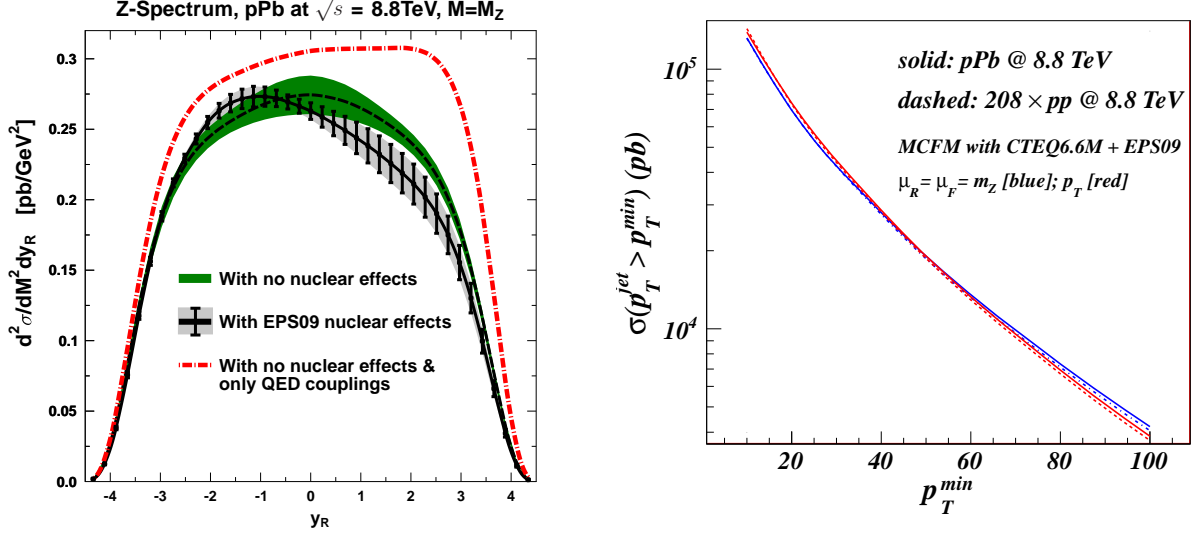

Fig. 3: *Left:* Rapidity distributions (in the centre-of-mass frame of the p+Pb collision) for dimuon pairs at the peak of the Z boson in p+Pb with and without nuclear effects in the PDFs — the corresponding bands correspond to the uncertainties in the proton PDFs and the nuclear PDFs as given by CTEQ6.6M [49] and EPS09 [25] respectively. For comparison, also the corresponding spectrum for only QED couplings (multiplied by a factor 1100) is shown by a red line — Figure from [43]. *Right:* Integrated cross section $\sigma(pp \to Z[\to \mu^+\mu^-]$+jet) as a function of the minimum transverse momentum of the leading jet, $p_T^{\min}$, with two different scale choices (upper curves at $p_T^{\min} = 10 \, \text{GeV} \, \mu_R = \mu_F = p_T$, lower curves $\mu_R = \mu_F = m_Z$).

In Fig. 3 *Left* we plot the rapidity distribution for the NLO production of dimuon pairs at the peak of the mass of the Z-boson in p+Pb collisions at LHC energies (notice that the rapidity refers to the p+Pb centre-of-mass frame and cross section is per nucleon). The fact that the isospin corrections are almost negligible for Z boson production yields a spectrum which is almost rapidity-symmetric before nuclear corrections to PDFs are implemented. This fact provides a clear advantage of the p+Pb system over the Pb+Pb system as forward-backward asymmetries provide direct information about the nuclear PDFs without the need for reference p+p data [43].

In Fig. 3 *Right* we plot the corresponding NLO inclusive cross section $\sigma(pp \to Z$+jet), for Z decaying into leptons, as a function of the minimum transverse momentum of the leading jet, $p_T^{\min}$. The cross section has been computed with the MCFM package [48] integrating the dimuon invariant mass region in the range $60 \, \text{GeV} < M_{\mu^+\mu^-} < 120 \, \text{GeV}$. This provides a realistic estimate of the experimental conditions for measuring the Z mesons at the LHC, as done, in particular in the corresponding measurement in Pb+Pb collisions from Ref. [41]. Nuclear effects are included using the parameterization of Ref. [25] and cross sections are absolute — for comparison, the p+p cross section at the same energy and scaled by the corresponding atomic number of the lead nucleus is also shown. In this integrated cross sections, the nuclear effects on the integrated cross sections were found to be small and are difficult to disentangle from the typical theoretical uncertainties of the NLO calculation. More differential distributions are

expected to provide further tests of the nuclear PDFs.

Using the default luminosity quoted in this document, one would expect on the order of 4000 events with dimuons per unit rapidity in an integrated invariant mass region around the Z peak at midrapidity — see also [43] — and a factor of 2 smaller yields for the case of Z+1jet with $p_T^{\text{jet}} > 10$ GeV. The corresponding values decrease quickly with increasing p_T. For example, the yield with $p_T^{\text{jet}} > 60$ GeV is a factor of ~ 10 smaller. From these results it is clear that a minimum luminosity of $\sim 10^{29}$ cm^{-2}s^{-1} is required for these studies to be feasible. Moreover, in realistic experimental conditions, the efficiency in the reconstruction of jets would impose a limit on the minimum p_T. A factor of at least 10 more luminosity than the one reported in the previous section would be a prerequisite for high enough statistics in Z+jet measurements.

It is also worth noting that similar yields are expected in Pb+Pb collisions where no extra hot-matter effects are present for the production of electroweak bosons. The comparison of these two systems will cross-check the universality of the nPDFs and the Glauber model as well as precise studies of jet quenching in Z+jet events.

4.23 Photons

Prompt photon production cross sections have been computed in p+p collisions in QCD at NLO accuracy. We used for the computation the CT10 parton densities [50] and the Bourhis, Fontannaz and Guillet (BFG, set II) photon fragmentation functions [51, 52]. Fig. 4 (*Left*) shows the production cross sections at mid-rapidity for p+p collisions at $\sqrt{s} = 5.5$, 8.8 and 14 TeV. The theoretical uncertainties are estimated by simultaneously varying the renormalization, factorization and fragmentation scales from $p_T/2$ to $2\,p_T$ leading to a rather stable 20% systematic error.

Additional uncertainty should actually come from the rather poorly determined parton-to-photon fragmentation functions [51, 52, 53]. Although the fragmentation contribution to the photon cross section is about 20% or less for the fixed target energies, it can easily make up for about half of the observed photons at collider energies. An "isolation" cut of photon signal can help reduce significantly the less accurate fragmentation contribution [54]. Furthermore, the "isolation" cut can help improving the signal-to-background ratio because of the abundance of π^0's, which decay into two photons that could be misidentified as one photon at high momentum.

For the production cross sections in p+Pb collisions we use the same setup as in p+p collisions supplemented with different sets of nuclear PDFs. In Fig. 4 (*Right*) we present the nuclear modification ratios for the photon production cross section in p+Pb collisions over that in p+p collisions scaled by the atomic number of the lead nuclei. Also plotted is the ratio computed with proton PDFs but including the corrections due to the different quark content of the neutrons and the protons inside the Pb nuclei (isospin corrections). The effects are rather small over the entire range of transverse momentum studied.

As in previous cases, the p+p benchmark for photon production in p+Pb would need an interpolation from the lower energy and the top energy p+p runs. A potential experimental problem, which could lead to systematic uncertainties in the comparison, is the rapidity shift incurred for asymmetric collision systems.

Inclusive photon production will also be measured in Pb+Pb collisions at the LHC. The possible presence of additional hot-matter effects make the constraints on nuclear PDFs less
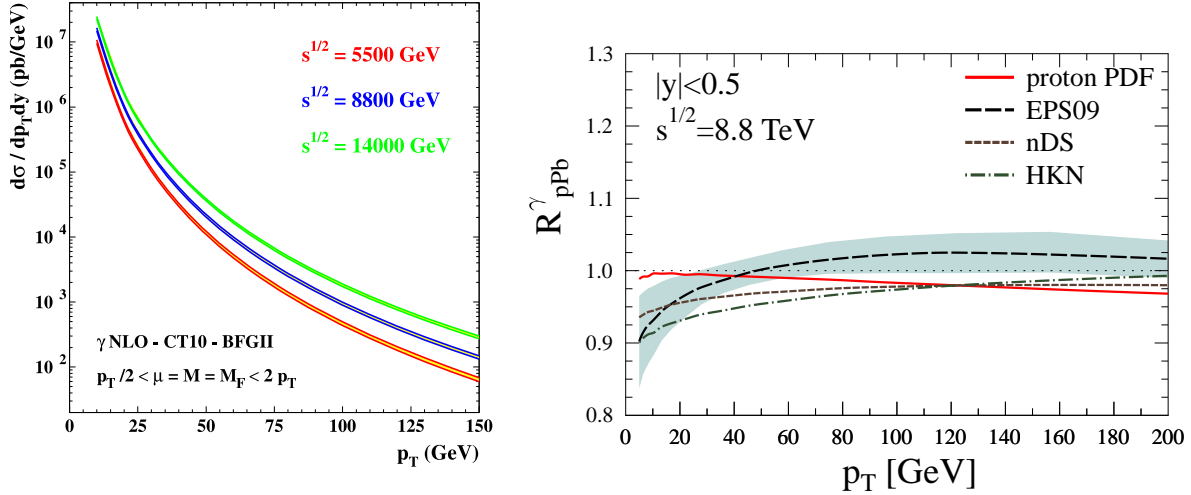
Fig. 4: *Left:* Prompt photon p_T spectra is computed in p+p collisions at $\sqrt{s} = 5.5, 8.8$ and 14 TeV. *Right:* Expected nuclear effects in the scaled ratio of p+Pb over p+p for different sets of nuclear PDFs, EPS09 [25], HKN07 [26] and nDS [27]. Also shown are the effect of the different isospin content of the nuclear and proton projectiles. Figure from [55].

stringent than in the p+Pb case as the actual size of these effects suffers from large uncertainties. Turning the argument around, a precise knowledge of the photon production in p+Pb collisions is a necessity to pin down the presence of additional effects in Pb+Pb which are not expected to be large.

Finally, we comment on typical counting rates in p+Pb collisions at $\sqrt{s} = 8.8$ TeV assuming a luminosity of $\mathcal{L} = 10^{29}$ cm^{-2} s^{-1}. While one could expect as many as 1.2 10^5 events at $p_T = 25$ GeV in a one month run, this rate decreases to 5000 events for 50 GeV photon. Still, such a luminosity would guarantee rather high precision measurements in the p_T range from 25 to 50 GeV.

4.24 Heavy flavor

The description of heavy quark production in hadronic collisions provided by the so-called FONLL (Fixed Order plus Next-to-Leading Log resummation) approach [56] has in recent years been shown to predict successfully bottom and, to a slightly lesser extent, charm cross sections in p+p collisions at RHIC and $p + \bar{p}$ collisions at the Fermilab Tevatron.

For this report we shall restrict ourselves to the small transverse momentum limit, our main goal being an assessment of nuclear shadowing effects in p+Pb collisions. In this limit FONLL coincides by construction with the NLO calculation [57]: it is therefore the latter which we shall use, complemented with non-perturbative fragmentation functions identical to those used in [58], and the EPS09 parameterization [25] of the shadowing effects implemented in the FONLL package for this purpose. The charm and bottom mass are set to 1.5 and 4.75 GeV respectively, and the CTEQ6.1 [38] proton parton distribution functions are employed.

The results are shown in Fig. 5 for both charm and bottom. In both cases the transverse momentum distributions and the nuclear modification ratio R_{pA} are plotted. The bands correspond to uncertainties only on the PDFs. In the case of the total spectra, they include the uncertainties for the proton and the nuclear PDFs in quadrature, while the ratios include only
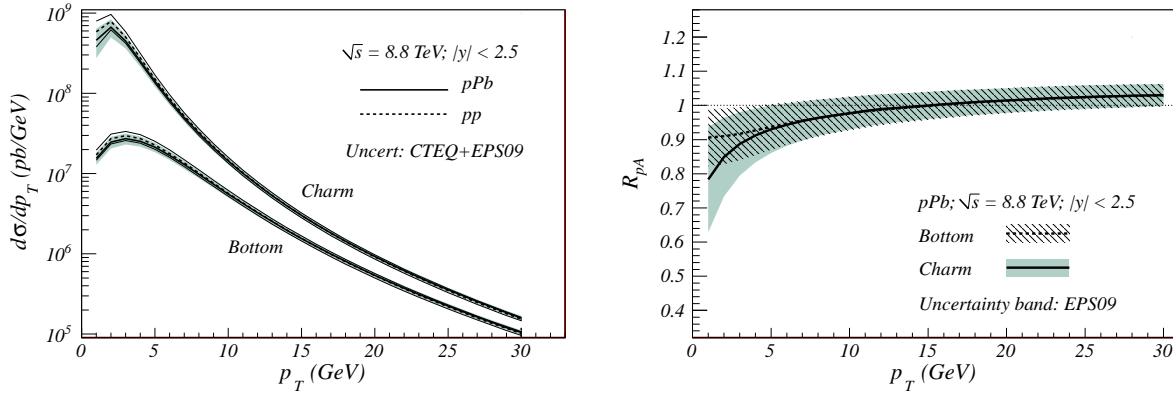
Fig. 5: *Left:* Charm and bottom production at the LHC in p+p and p+Pb collisions, as predicted by NLO QCD, complemented by EPS09 nuclear corrections where needed. Cross sections are per nucleon and uncertainties refer only to those from the PDFs (proton and nuclear ones added in quadrature). *Right:* Nuclear modification factors for both charm and bottom together with the corresponding uncertainties as given by the EPS09 set of nPDFs.

those from EPS09 — this procedure is explained in Ref. [25]. Although the nuclear effects are not very large, we note that the associated uncertainties are of the same order as the effects themselves. Hence, the additional effects expected in Pb+Pb collisions would necessitate the p+Pb control experiment for a precise interpretation.

4.25 Quarkonium

The calculation of quarkonium cross sections in the color evaporation model is described in Refs. [8, 59]. The total yield of lepton pairs from quarkonia decays in p+Pb collisions at $\sqrt{s} = 8.8$ TeV and nominal integrated luminosity is 3.9×10^7 inclusive J/ψ and 2.5×10^5 inclusive Υ [8].

We have included intrinsic transverse momentum, k_T, broadening on the quarkonium p_T distributions. We found that $\langle k_T^2 \rangle$ value of 2.5 GeV^2 is needed for agreement with the Tevatron data. A simple logarithmic dependence on the energy, $\langle k_T^2 \rangle_p = 1 + (1/6)\ln(s/s_0)$ GeV^2 with $\sqrt{s_0} = 20$ GeV, can account for the increase with increasing $\sqrt{s}$. Thus for $\sqrt{s} = 8.8$ TeV, $\langle k_T^2 \rangle_p = 3.03$ GeV^2. The k_T broadening due to the presence of nuclear matter is applied as in Ref. [60].

Sample J/ψ and Υ p_T distributions in 8.8 TeV p+p and p+Pb collisions at the LHC are shown in Fig. 6 in the central region, $|y| \leq 1$ and the forward region $3 < y < 4$. The broadening of the p_T distributions in p+Pb collisions is rather small. The effects of initial-state shadowing on the p_T distribution, included using the EKS98 parameterization, are likely to be more important.

The low p_T shadowing effect on the rapidity distributions can be rather substantial at low x. High p_T is less affected. In addition to the EKS98 parameterization in the dashed histogram, the nDS (dot-dashed) and EPS08 (dotted) shadowing parameterizations are also shown on the right-hand side of Fig. 6. Note that at backward rapidity (larger x for the nucleus assuming the Pb beam moves right to left), the curves tend to coincide with the p+p curve although the strong anti-shadowing of EPS08 manifests itself for the Υ at $y < -3$. The deviations from the p+p baseline become stronger with increasing y (smaller x). The nDS parameterization of the gluon distribution gives the weakest effect while the EPS08 parameterization is strongest.
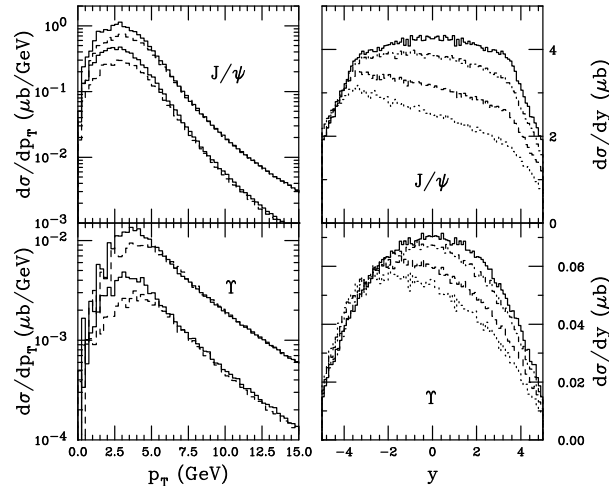
Fig. 6: The inclusive J/ψ (top) and Υ (bottom) p_T (left) and y (right) distributions, calculated in the color evaporation model for p+p (solid) and p+Pb (dashed) collisions at 8.8 TeV. The p_T distributions are calculated using the MRST PDFs and, in p+Pb, the EKS98 shadowing parameterization. They are shown for the central ($|y| < 1$) and forward ($3 < y < 4$) rapidity regions. The forward curves are divided by a factor of 5 for clarity. The rapidity distributions at 8.8 TeV are shown for the p+p baseline and p+Pb collisions with the nDS (dot-dashed), EKS98 (dashed) and EPS08 (dotted) shadowing parameterizations. Notice that all cross sections are per nucleon and rapidity refers to the centre-of-mass frame of the p+Pb system.

(Note that the rapidity shift of the p+Pb center of mass is not shown on the plot.) For a complete discussion of the effects of shadowing and nucleon absorption in d+Au and p+A collisions as a function of rapidity and centrality, see Ref. [61]. For recent results on the rapidity dependence of cold matter effects at the LHC, including calculations with the EPS09 shadowing parameterization, see Ref. [62].

From these results it is clear that any conclusion about the effects observed in Pb+Pb collisions on quarkonia production need the p+Pb benchmark.

In summary, the luminosity quoted in this document is sufficient for unique studies of perturbative observables. The cases of electroweak boson or photon production will suffer from a smaller luminosity. The two main issues to overcome are the c.m. energy interpolations (between the energies of the A+A and p+A runs) and the rapidity shifts. For the later, i.e. for those observables for which acceptance is the limiting factor, more specific studies would be required and collider operations in the A+p as well as the p+A modes are needed.

5. NEW PHYSICS OPPORTUNITIES: TESTING PERTURBATIVE SATURATION

Parton saturation [63] is expected to occur at low values of Bjorken x — i.e. when the gluon density inside protons and nuclei becomes large. It can be described by an effective theory derived from QCD: the Color Glass Condensate (CGC) — see e.g. [64] for a recent review — which generalizes the BFKL evolution equation [65, 66] to situations where the large density of gluons leads to non-linear effects such as recombination. Searches have been made for the evidence of parton saturation effects in small-x data from lepton-proton or lepton-nucleus collisions as well as in RHIC data from Au+Au and d+Au systems. Although with the last theo-

retical developments the agreement with experimental results is rather good, no firm evidence of the relevance of saturation physics has been found partly because the usual DGLAP approaches still provide a very successful description of the data also in the small-x region.

Rather general geometrical considerations make saturation effects larger in nuclei by a factor $\sim A^{1/3}$ as compared to the proton. As a result, if $x_{\text{sat,p}}$ is a typical value at which non-linear effects appear at a given scale Q_{sat}^2 in the proton, the corresponding value for a nucleus is larger, $x_{\text{sat,A}} \sim A^{\frac{1}{3\lambda}} x_{\text{sat,p}}$, for a gluon distribution behaving as $x^{-\lambda}$. This fact makes nuclear collisions especially suitable for the study of parton saturation physics.

The bulk of particle production in nucleus-nucleus collisions has been computed using methods from the CGC and, in fact, this approach has been rather successful in predicting the measured Pb+Pb multiplicities at the LHC [67]. Heavy-ion collisions, however, are not a very good testbed if one is interested in the study of saturation phenomena *per se*. Indeed, in these collisions final state effects appear which complicate the study of properties of the wave-function of the incoming projectiles. To take an extreme view, if the system formed in nucleus-nucleus collisions reaches a state of local thermal equilibrium, then by definition it has no memory of its early stages beyond inclusive properties such as the energy density and perhaps some long-range correlations in rapidity.

The cleanest experimental situation to look for saturation physics would be in nuclear DIS experiments at the highest possible energies. There, one would have direct access to the small-x region of phase space. HERA experiments so far provide the smallest values of x with protons, $x \gtrsim 10^{-5}$ for $Q^2 \gtrsim 1$ GeV^2, while nuclear data reaches $x \sim 10^{-2}$ at most. New proposals such as the EIC or the LHeC [10, 11] could extend these ranges significantly. However, there will be no overlap in time with the LHC nuclear programme, at least not in the coming next ten years. Therefore, proton-nucleus collisions at the LHC offer a unique opportunity to study the physics of gluon saturation. The smallest possible values of x in nuclei can be studied at forward rapidities and with final states that have a moderate transverse mass.

Several different observables have been proposed as good probes of the saturation of partonic densities. In most of them only one universal object appears, the so-called "dipole cross-section". This universality can be checked by different measurements at the LHC and by comparing to smaller energies, in particular with RHIC and with HERA data.

Here, we shall not review the different predictions expected from the saturation of parton densities. A general effect is that the presence of non-linear terms in the evolution equations diminish the growth in the corresponding observables relative to the linear case. Another generic property of the present implementations is a correspondence between the rapidity- and $\sqrt{s}$-dependencies of the non-linear effects which will be testable in p+A collisions at the LHC. Naively, the effects at $y_{\text{LHC}} \sim 0$ are expected to be similar to those at $y_{\text{RHIC}} \sim 3.5$. In order to visualize this fact, we compare in Fig. 7 the nuclear effects in inclusive hadron production computed in collinear factorization [68] with a calculation which uses dipole cross sections evolved with non-linear Balitsky-Kovchegov (BK) equations including running coupling effects [69]. The last framework is able to reproduce RHIC data at forward rapidities. Although the BK approach used here is expected to break at a certain value of the transverse momentum, the large differences between the two predictions and the large p_T-range available at the LHC will allow to identify a window where the two scenarios could be cleanly discriminated. It is worth noting here that, at variance with the collinear factorization approach where the hard cross section is computed, the CGC approach provides only the spectra of produced particles. This limitation can be traced back to the fact that dipole amplitudes are distributed in transverse position and

need to be integrated while this integration is implicit in the PDFs obtained in the collinear factorization. In this situation, the computation of the ratios needs information external to the theoretical framework of the CGC about the inelastic p+p and p+A cross sections, or, alternatively, about the average number of nucleon-nucleon collisions $\langle N_{\mathrm{coll}} \rangle$, usually computed in the Glauber model. This additional ingredient translates into a normalization factor in the ratio $R_{pA}(p_T, \eta)$ — $\langle N_{\mathrm{coll}} \rangle$ has been fixed to be the same as for RHIC in Fig. 7 but could be larger at the LHC. If the presence of saturation effects turns out to be a matter of precision, e.g. compatibility of different data sets within a global fit in either a DGLAP or a CGC approach, a good control over the normalization cross sections and/or the validity of the Glauber model is needed.
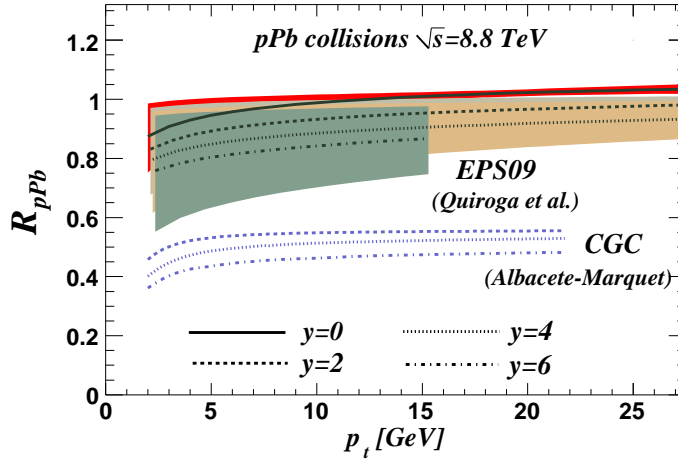

Fig. 7: Nuclear modification factor for inclusive charged hadrons in p+Pb collisions for different rapidities — notice, centre-of-mass rapidities here — computed in the saturation approach of [69] compared with the same quantity computed in collinear factorization [68] using EPS09 nuclear PDFs [25], including the corresponding uncertainty bands — notice that they overlap in most of the p_T-region plotted. As explained in the text, the total normalization of the CGC calculation is proportional to the $\langle N_{\mathrm{coll}} \rangle$ computed within the Glauber model. For this particular case, this quantity has been fixed to the one computed by the BRAHMS experiment for RHIC conditions, $\langle N_{\mathrm{coll}} \rangle = 3.6$.

Another generic feature of the presence of saturation of partonic densities is the modification of particle correlations due to collective effects in the initial wave function. In the extreme case, the momentum imbalance of one given particle can be shared among a large number of other particles, leading to a loss of the correlation signal. Preliminary data from RHIC [70] find such a decorrelation, compatible with a calculation in saturation physics [71], although alternative explanations have also been put forward [72].

The present status of the phenomenological calculations within the CGC framework have strongly benefited from the inclusion of NLO terms in the corresponding BK evolution equations. These terms are essential to make the comparison with experimental data meaningful at the quantitative level and to convert this framework into a predictive tool for which the p+A programme at the LHC will provide ideal testable conditions. Improvements in the limitations of the formalism mentioned above are being worked out and have partly already been used [73] in the description of the centrality dependence of multiplicities in Pb+Pb collisions measured by ALICE [67].

6. OTHER OPPORTUNITIES

6.1 Ultra-peripheral Collisions

Charged hadrons accelerated at very high energies generate strong electromagnetic fields, equivalent to a flux of quasi-real photons, which can be used to study high-energy $\gamma + \gamma$, γ+p and γ+A processes in ultraperipheral collisions (UPCs) where the colliding systems pass close to each other without interacting hadronically. The effective photon flux, which can be translated into an effective luminosity, is proportional to the square of the charge, Z^2, and thus significantly enhanced for heavy ions. The figure of merit for photoproduction is the effective γ+A luminosity, $\mathcal{L}_{AB}\, n(\omega)$, where $\mathcal{L}_{AB}$ is the accelerator luminosity and $n(\omega)$ is the photon flux per nucleus. Figure 8(a) compares $\mathcal{L}_{AB}n(\omega)$ for γ+p and γ+Pb collisions in p+Pb interactions to the case where the photon is emitted from an ion in a Pb+Pb collision. Figure 8(b) compares the same quantity for $\gamma + \gamma$ collisions.
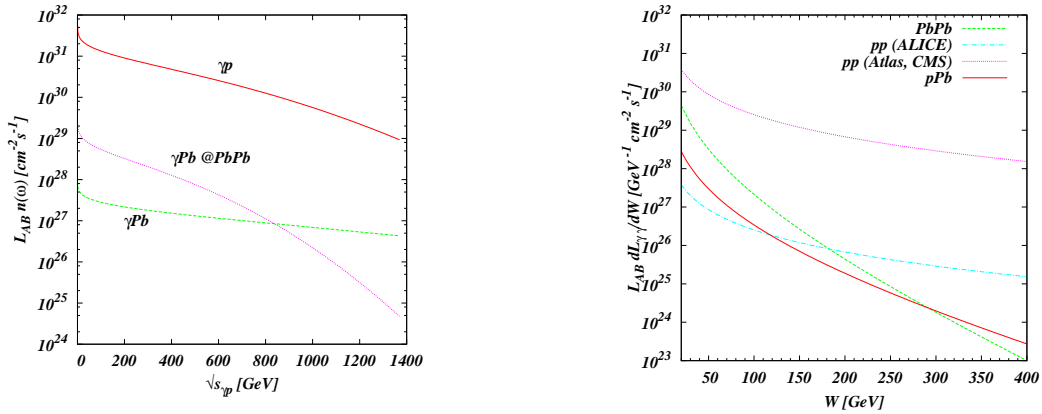

Fig. 8: *Left:* Effective γ+A luminosity $\mathcal{L}_{AB}\, n(\omega)$ for three cases at the LHC: the photon is emitted from the proton (labeled γPb), from the ion (γp), and from the ion in a Pb+Pb collision (γPb@Pb+Pb). *Right:* Effective two-photon luminosities $\mathcal{L}_{AB}(d\mathcal{L}_{\gamma\gamma}/dW_{\gamma\gamma})$ for p+p, p+Pb and Pb+Pb collisions at the LHC.

UPCs in p+A collisions present advantages with respect to both ultraperipheral A+A and p+p collisions. First, relative to A+A collisions, the p+A luminosities are three orders of magnitude larger, and the hadronic center-of-mass energies are also larger. Moreover, the $\gamma + \gamma$ centre-of-mass energies are also higher, resulting from a harder proton photon spectrum and a smaller distance between the centers of the radiating charges. In addition, it is easier to remove other photoproduction backgrounds than in A+A collisions characterized by additional photon exchanges which lead to forward neutron emission. It is also possible to tag the scattered proton using Roman Pot detectors (CMS/TOTEM [74], ATLAS/ALFA [75], FP420 [76]), allowing full kinematic reconstruction by separating the momentum transfers from the proton and the ion. The advantage of p+A with respect to p+p UPCs is threefold. First, the photon flux of one beam increases by Z^2. It is also possibile to trigger on and carry out measurements with almost no event pileup and also remove most of the exclusive diffractive backgrounds. Since the nucleus is a fragile object, Pomeron-mediated interactions in p+A collisions will, at variance with p+p, almost always lead to the emission of a few nucleons detectable in the zero degree calorimeters.

The interest in UPCs at the LHC includes QCD studies such as probing the low-x gluon distributions in protons and nuclei, beyond the reach of HERA and RHIC respectively, via inclusive and exclusive dijet, heavy-flavour and vector meson measurements; as well as elec-

troweak processes and new physics searches [77, 78, 79]. An extensive report on the physics of UPCs at the LHC is available in Ref. [80]. UPC studies are integral part of the ALICE [81, 82], ATLAS [83] and CMS [84] heavy-ion programmes.

6.11   Physics potential of photon-proton/nucleus physics

Ultraperipheral p+A collisions will play a dual role in both extending studies of the hadron structure to a new kinematic domain and serving as a reference for similar studies in ultraperipheral A+A collisions.

Inclusive photonuclear processes are of particular interest for the study of small-x parton densities. Dijet [85], heavy flavor [86] and quarkonia photoproduction can be used to extract small-x gluon densities in protons and nuclei. At comparable virtualities, LHC measurements will extend those at HERA to an order of magnitude smaller x. For example, the b quark rate in p+Pb collisions is measurable to $x \sim 10^{-4}$ at $p_T \sim 5$ GeV [87]. The c quark rate could be measured at even smaller x by going to lower p_T. Comparison of the rapidity dependence of leading charm in γ+A and γ+p scattering will be a very sensitive test of the onset of the nonlinear regime.

Exclusive photoproduction of heavy quarkonia, $\gamma + A(p) \rightarrow V + A(p)$, where $V = J/\psi, \Upsilon$ and the nucleus A or proton p remains intact) offers a useful means to constrain the small-x nuclear gluon density down to values $x = m_V^2/W_{\gamma+A,p}^2$. The mass, M_V, and rapidity, y, of the final-state vector meson can be used to determine the photon energy, ω, in the laboratory frame from $y = \ln(2\omega/M_V)$. This determination is ambiguous in A+A collisions as it is not possible to distinguish which nucleus emitted the photon and which was the target, and thus it is only possible to convert $d\sigma/dy$, into $\sigma(\gamma + A \rightarrow V + A)$ (in the nuclear target frame) for a single photon energy corresponding to $y = 0$. This ambiguity is avoided in p+A collisions because the photon is most frequently emitted by the heavier nucleus. Thus measuring $d\sigma/dy$ as a function of y corresponds to measuring the energy dependence of the photoproduction cross section.

Exclusive vector meson photoproduction has been studied in UPCs at RHIC by STAR [88, 89, 90, 91] and PHENIX [92, 93]. The LHC p+A measurements would be extremely valuable as a 'benchmark' for understanding similar UPC A+A data and measuring nuclear shadowing. The ratio of cross sections $\sigma(\gamma + A \rightarrow V + A)/[A \cdot \sigma(\gamma + p \rightarrow V + A)]$ at the same $W_{\gamma+N}$ allows for a rather direct measurement of nuclear shadowing. The A+A data provides the numerator while the p+A data are used in the denominator. Many theoretical and experimental systematic uncertainties cancel in the ratio.

Last but not least, the cross section for the electromagnetic proton dissociation reaction in the field of the nucleus, p+Pb $\rightarrow$ Pb+X, can be reliably calculated ($\pm 5\%$ uncertainties) and thus usable as "luminometer". Ultraperipheral d+Au interactions along with electromagnetic deuteron dissociation have been measured at RHIC, with a cross section of $\sigma_{\text{EMD dAu}} = 1.99$ b [94], and compared to theoretical predictions [95] to directly determine the luminosity needed to calibrate the cross sections of other processes produced in d+Au collisions [96].

6.12   Physics potential of two-photon and electroweak processes

Photon-photon interactions in UPCs at LHC energies can access a rich QCD, electroweak, and even beyond the Standard Model (BSM) programme at the TeV scale. In the QCD sector, double vector meson production $\gamma + \gamma \rightarrow V + V$ [78], will be accessible with similar rates in p+A and A+A collisions. In addition heavy flavor meson spectroscopy can distinguish between

quark and gluon-dominated resonances, search for glueballs [77, 78], and study η_c spectroscopy through radiative J/ψ decays with larger rates than in direct $\gamma + \gamma$ production [79].

QED dilepton production is also of interest as a luminosity monitor [97]. In CMS [74], the CASTOR/TOTEM forward detectors can measure low-p_T e^+e^- pairs, corresponding to large impact parameters, where theoretical calculations are most reliable. Higher-order QED corrections are expected to reduce the huge dielectron cross sections in Pb+Pb UPCs ($\sigma_{ee} \approx$ 200 b). The p+Pb data could provide experimental verification of the predicted deviations from the Z^4 scaling expected for symmetric ion-ion collisions, as yet unobserved at RHIC or the SPS.

Tagging forward protons at the LHC with Roman Pots will enhance the detection capability of electroweak processes, improving the background suppression. The addition of far-forward detectors at ± 420 m [76] would improve forward light-ion detection, allowing p+A events to be double tagged. A process well suited to testing the electroweak (γWW) gauge boson self-interaction is single W photoproduction [98] from a nucleon in ultraperipheral p+A and A+A [99] collisions. Similarly, 10 $\gamma + \gamma \rightarrow W^+ + W^-$ events are expected in a 10^6 s p+A run. These W^+W^- pairs, characterised by small pair p_T, are sensitive to the quartic gauge boson couplings. Lastly, even Higgs boson production would be measurable if the p+A luminosity were increased by a factor of 60 [100].

6.2 Measurements of Interest to Astroparticle Physics

Current cosmic-ray data reveal a rapid increase of the average mass number $\langle A \rangle$ of the cosmic-ray flux — i.e. a transition from lighter (p, He,...) to heavier composition — in the energy range around $\sim 10^{15}$ eV in the laboratory frame, coinciding with a steepening of the cosmic-ray flux. In the energy range around $\sim 10^{18}$ eV there are indications that the composition becomes lighter again, correlated with a hardening of the spectral slope of the cosmic-ray flux [101]. The most recent data from the Pierre Auger Observatory points to yet another change back to a heavier composition in the highest energy range $\sim 10^{19}$ eV [102]. A precise determination of this quantity would have a profound impact on the knowledge of the sources of the high-energy cosmic rays.

Direct measurements of the cosmic-ray mass number A are possible only up to $E < 10^{15}$ eV. Above this energy attempts to infer the A of the primary particle are based on the measurements of the extensive air shower (EAS) induced when the cosmic ray interacts upon entering the atmosphere. The main source of uncertainty in the predictions of the EAS observables stems from our limited knowledge of the features of hadronic interactions in this energy range, in particular at forward rapidities, where most of the energy of the shower flows. In fact, none of the existing hadronic interaction models currently used for modeling EAS development [103, 104, 105] is able to provide a consistent and satisfactory description of cosmic-ray data due to the unconstrained extrapolations from energies reached at accelerator based experiments. In this situation, data from the LHC helps to constrain these models and to improve the interpretation of cosmic ray measurements [106]. In particular, a proton-nucleus run would be of utmost importance since the EAS are predominantly generated in collisions of the cosmic-rays with Nitrogen and Oxygen nuclei in the upper atmosphere. The measurements of particle production at very forward rapidities, accessible to existing LHC detectors such as the Zero-Degree-Calorimeters [107] and the LHCf [108] experiment, are therefore of special importance.

7. EXPERIMENTAL CONSIDERATIONS

In Fig. 9 the expected kinematical regions measured in the (x, Q^2) plane for different processes[3] accessible with an integrated luminosity of 0.1 pb^{-1} in a p+Pb run are plotted inside the band indicating the maximum kinematical reach. Also shown in the same figure is the reach of the current data used to constrain the present knowledge of nuclear PDFs. The rest of the phase space to be studied at the LHC is basically unconstrained with regard to nuclear effects. Notice that the band corresponding to RHIC kinematics has to be compared with the total kinematic reach of the LHC, as the region accessible with actual processes, is, in fact, much smaller [109]. This clearly illustrates the wide new region opened at the LHC for both benchmarking perturbative processes in A+A collisions, and for the new physics opportunities discussed in this report.
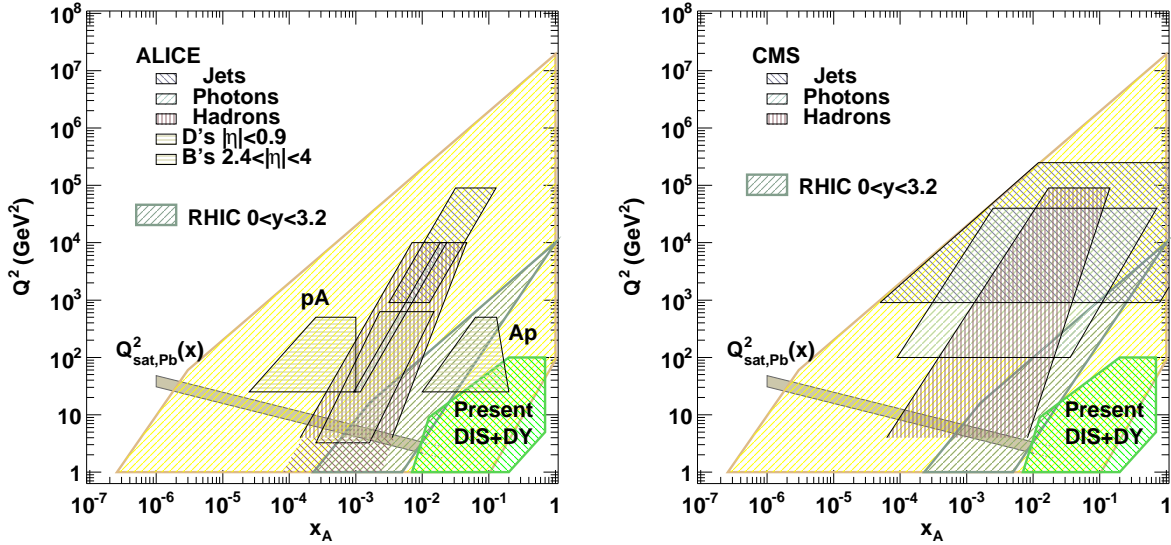
Fig. 9: Total kinematical reach of p+Pb collisions at $\sqrt{s}$ =8.8 TeV at the LHC. Also shown is the reach with an integrated luminosity of 0.1 pb^{-1} for some of the particular probes studied in the present document for ALICE and CMS, respectively.

The LHC detectors are designed to run under the much more demanding conditions of Pb+Pb and high-luminosity p+p collisions. Extensive studies of the detector capabilities and performance, including p+A runs, are available [81, 82, 84, 83], which include discussion of the centrality determination in p+A and performance for various observables. We focus here on topics related to the rapidity shifts and the energy interpolations for benchmarking as well as the need of p+A and A+p collisions during the same running period. The luminosity quoted in this document, $\mathcal{L} = 10^{29}$cm^{-2}s^{-1}, is expected to be sufficient to carry out the proposed measurements and matches the detector capabilities. Assuming an effective running time of 10^6 s, the total integrated luminosity is 0.1 pb^{-1}. Any significant reduction of this quantity would significantly impair the measurement of some of the observables — e.g. electroweak boson (γ, W and Z) production — for benchmarking or other physics studies as explained previously in the text. On the other hand, a larger luminosity would allow one to measure with

---

[3] These limits correspond to $2 \rightarrow 2$ or $2 \rightarrow 3$ processes. If $2 \rightarrow 1$ kinematics is relevant, as e.g. in Drell-Yan production or in inclusive hadron production in the CGC approach, the relevant values of x may become significantly smaller.

high enough precision other relevant observables such as Z+jet, important for jet calibration in jet quenching measurements and for nPDF studies.

Benchmarking in p+A is essential for all perturbative studies relevant for the Pb+Pb programme at the LHC. The usual procedure is to study ratios between the A+A or p+A cross sections with the corresponding p+p one scaled by the appropriate factor. This is, in principle, the same procedure to be used at the LHC. One of the questions is how to produce such ratios, when the energy of the collision is different for different colliding systems, as it is the case for the top LHC energies in p+p, p+A and A+A. Ideally, benchmarking p+p runs at the same energy have to be done. This possibility has been explored in a short p+p run at $\sqrt{s_{\mathrm{NN}}} = 2.76$ TeV in 2011 with an integrated luminosity of around 20 nb^{-1} for ALICE and about a factor of 10 larger for CMS and ATLAS. These luminosities are of the same order as the ones considered here and should provide the needed conditions for benchmarking without theoretical input. In the absence of p+p data at the same energy as the Pb+Pb or the p+Pb runs, interpolations among different energies will be needed through a ratio of the type [110]

$$\sigma(pp \to X; \sqrt{s_{\mathrm{PbPb/pPb}}}) = \frac{\sigma^{\mathrm{TH}}(pp \to X; \sqrt{s_{\mathrm{PbPb/pPb}}})}{\sigma^{\mathrm{TH}}(pp \to X \sqrt{s_{pp}})} \sigma^{\mathrm{EXP}}(pp \to X; \sqrt{s_{pp}}). \tag{6}$$

where X depends on the process under consideration[4]. However, the accuracy of this interpolation is process dependent. Uncertainties are quite small $\mathcal{O}(5\%)$ for the hardest processes, e.g. electroweak boson production, but are usually larger otherwise. For example they are 12% (8%) in charm (beauty) production when extrapolating from $\sqrt{s} = 14$ TeV down to $\sqrt{s} = 5.5$ TeV [82]. At the time of the p+A run some of these uncertainties could be further reduced through constraints arising from the p+p program.

Different observables could need slightly different benchmarking strategies depending on the theoretical or experimental capabilities to isolate different nuclear effects if present — for example modifications in the hadronization. For those effects solely depending on a modification of the PDFs in the nuclear environment, the use of ratios with respect to p+p and the corresponding interpolation (6) is strictly speaking not essential, especially if quantities not depending on the knowledge of the proton PDFs can be built, see e.g. [43]. In general the same consideration applies for factorization in the fragmentation functions when computing e.g. inclusive particle production at high transverse momentum. In this case, good control over the normalization of the cross sections would significantly improve the comparisons as well as allow for precision checks of the Glauber model.

In this document a canonical energy for a p+Pb run of $\sqrt{s} = 8.8$ TeV has been considered. This means that a second interpolation to the Pb+Pb maximum energy will be necessary. The potential problem for this second interpolation lies on the possible energy dependence of effects which are not factorizable in terms of nuclear PDFs. With the present knowledge from RHIC and SPS, this will be especially relevant for quarkonia production — in this case a p+Pb run at the same energy of the Pb+Pb one would be preferred. For other observables such effects are not expected. For nuclear PDF studies and for the new physics opportunities quoted in this document, the highest energy run would be more interesting, also for a reduced systematic uncertainties, if p+p data at the same energy are not available. Notice that constraints for PDFs in a given range of x are stronger if the kinematical limit is not reached.

A second independent effect which needs to be taken into account is the rapidity shift. This rapidity shift, $\Delta y = 0.46$, will be present irrespectively of the energy of the p+Pb run. This

---

[4]For a first study with experimental data on the relevance of these extrapolations see e.g. [3].

is especially relevant for detectors which are not symmetric in rapidity. In that case, the ideal running conditions for benchmarking would be to have both p+A and A+p collisions during the same running period. A fast enough switch between the two modes would, in this case, be a requirement for a successful run.

The integrated luminosity used in this document for benchmarking purposes is 0.1 pb^{-1}. Any substantial reduction of this quantity would alter the performance of some of the measurements presented here, in particular those involving electroweak processes and large virtualities as mentioned above. A luminosity larger by a factor of ~ 10, on the other hand, would give access to new important observables.

References

[1] K. Aamodt *et al.* [ALICE Collaboration], Phys. Rev. Lett. **105** (2010) 252301 [arXiv:1011.3916 [nucl-ex]].

[2] K. Aamodt *et al.* [ALICE Collaboration], arXiv:1011.3914 [nucl-ex].

[3] K. Aamodt *et al.* [ALICE Collaboration], Phys. Lett. B **696** (2011) 30 [arXiv:1012.1004 [nucl-ex]].

[4] G. Aad *et al.* [ATLAS Collaboration], Phys. Rev. Lett. **105** (2010) 252303 [arXiv:1011.6182 [hep-ex]].

[5] S. Chatrchyan *et al.* [CMS Collaboration], arXiv:1102.1957 [nucl-ex].

[6] A. Accardi *et al.*, Chapter 1: *(pdf's, shadowing and pA collisions)* of the CERN Yellow Report on Hard probes in Heavy-Ion Collisions at the LHC, CERN-2004-009 [arXiv:hep-ph/0308248].

[7] A. Accardi *et al.*, Chapter 2 *(Jet Physics)* of the CERN Yellow Report on Hard probes in Heavy-Ion Collisions at the LHC, CERN-2004-009 [arXiv:hep-ph/0310274].

[8] M. Bedjidian *et al.*, Chapter 3: *(Heavy flavour Physics)* of the CERN Yellow Report on Hard probes in Heavy-Ion Collisions at the LHC, CERN-2004-009 [arXiv:hep-ph/0311048].

[9] F. Arleo *et al.*, Chapter 4: *(Photon Physics in heavy ion collisions at the LHC)* of the CERN Yellow Report on Hard probes in Heavy-Ion Collisions at the LHC, CERN-2004-009 [arXiv:hep-ph/0311131].

[10] N. Armesto *et al.*, LHeC Conceptual Design Report: Physics at High Parton Densities; in preparation.

[11] B. Surrow, J. Phys. Conf. Ser. **110** (2008) 022049.

[12] O.S. Brüning, P. Collier, P. Lebrun, S. Myers, R. Ostojic, J. Poole, and P. Proudlock (editors), *LHC Design Report Vol. I: the LHC main ring,* CERN-2004-003-V1, 2004.

[13] T. Satogata et al., Proceedings of the 2003 Particle Accelerator Conference, Portland Oregon, pp. 1706-8 2003.

[14] C.J. Gardner et al., Proceedings of the 2008 European Particle Accelerator Conference, Genoa Italy, pp. 2548-50, 2008.

[15] J.M. Jowett and C. Carli, *The LHC as a proton-nucleus collider*, Proceedings of the 2006 European Particle Accelerator Conference, Edinburgh, Scotland, pages 550–552, 2006.

[16] H.G. Hereward and S. Myers, CERN ISR Performance Report, *Overlap knock-out* 12.8.1975,
`http://cdsweb.cern.ch/record/1131029/files/CM-P00072051.pdf`
and later references.

[17] S. S. Adler *et al.* [PHENIX Collaboration], Phys. Rev. Lett. **91** (2003) 072303 [arXiv:nucl-ex/0306021].

[18] J. Adams *et al.* [STAR Collaboration], Phys. Rev. Lett. **91** (2003) 072304 [arXiv:nucl-ex/0306024].

[19] S. S. Adler *et al.* [PHENIX Collaboration], Phys. Rev. Lett. **91** (2003) 072301 [arXiv:nucl-ex/0304022].

[20] C. Adler *et al.* [STAR Collaboration], Phys. Rev. Lett. **89** (2002) 202301 [arXiv:nucl-ex/0206011].

[21] A. Adare *et al.* [PHENIX Collaboration], Phys. Rev. Lett. **98** (2007) 232301 [arXiv:nucl-ex/0611020].

[22] M. C. Abreu *et al.* [NA50 Collaboration], Phys. Lett. B **477** (2000) 28.

[23] J. C. Collins, D. E. Soper and G. Sterman, Adv. Ser. Direct. High Energy Phys. **5** (1988) 1.

[24] R. J. Glauber and G. Matthiae, Nucl. Phys. B **21** (1970) 135.

[25] K. J. Eskola, H. Paukkunen, C. A. Salgado, JHEP **0904** (2009) 065. [arXiv:0902.4154 [hep-ph]].

[26] M. Hirai, S. Kumano, T. -H. Nagai, Phys. Rev. **C76** (2007) 065207. [arXiv:0709.3038 [hep-ph]].

[27] D. de Florian and R. Sassot, Phys. Rev. D **69**, 074028 (2004) [arXiv:hep-ph/0311227].

[28] K. Kovarik, *et al.*, Phys. Rev. Lett. **106**, 122301 (2011). [arXiv:1012.0286 [hep-ph]].

[29] H. Paukkunen, C. A. Salgado, JHEP **1007** (2010) 032. [arXiv:1004.3140 [hep-ph]].

[30] [CMS Collaboration], arXiv:1102.5435 [nucl-ex].

[31] V. Guzey, M. Strikman, Phys. Lett. **B687** (2010) 167-173. [arXiv:0908.1149 [hep-ph]].

[32] I. Arsene *et al.* [BRAHMS Collaboration], Phys. Rev. Lett. **93** (2004) 242303 [arXiv:nucl-ex/0403005].

[33] K. J. Eskola, H. Paukkunen, C. A. Salgado, JHEP **0807** (2008) 102. [arXiv:0802.0139 [hep-ph]].

[34] V. Khachatryan *et al.* [CMS Collaboration], JHEP **1009** (2010) 091 [arXiv:1009.4122 [hep-ex]].

[35] S. Frixione, Z. Kunszt and A. Signer, Nucl. Phys. B **467** (1996) 399 [arXiv:hep-ph/9512328].

[36] S. Frixione, Nucl. Phys. B **507** (1997) 295 [arXiv:hep-ph/9706545].

[37] S. Frixione and G. Ridolfi, Nucl. Phys. B **507** (1997) 315 [arXiv:hep-ph/9707345].

[38] D. Stump, J. Huston, J. Pumplin, W. K. Tung, H. L. Lai, S. Kuhlmann and J. F. Owens, JHEP **0310** (2003) 046 [arXiv:hep-ph/0303013].

[39] K. J. Eskola, V. J. Kolhinen and P. V. Ruuskanen, Nucl. Phys. B **535** (1998) 351 [arXiv:hep-ph/9802350].

[40] K. J. Eskola, V. J. Kolhinen and C. A. Salgado, Eur. Phys. J. C **9** (1999) 61 [arXiv:hep-ph/9807297].

[41] G. Aad *et al.* [ATLAS Collaboration], Phys. Lett. B **697** (2011) 294 [arXiv:1012.5419 [hep-ex]].

[42] R. Vogt, Phys. Rev. C **64** (2001) 044901 [arXiv:hep-ph/0011242].

[43] H. Paukkunen, C. A. Salgado, JHEP **1103** (2011) 071. [arXiv:1010.5392 [hep-ph]].

[44] P. B. Arnold and M. H. Reno, Nucl. Phys. B **319** (1989) 37 [Erratum-ibid. B **330** (1990) 284].

[45] R. J. Gonsalves, J. Pawlowski and C. F. Wai, Phys. Rev. D **40** (1989) 2245.

[46] W. T. Giele, E. W. N. Glover and D. A. Kosower, Nucl. Phys. B **403** (1993) 633 [arXiv:hep-ph/9302225].

[47] J. Campbell, R. K. Ellis, F. Maltoni and S. Willenbrock, Phys. Rev. D **69** (2004) 074021 [arXiv:hep-ph/0312024].

[48] J. M. Campbell and R. K. Ellis, Phys. Rev. D **62** (2000) 114012 [arXiv:hep-ph/0006304].

[49] P. M. Nadolsky *et al.*, Phys. Rev. D **78** (2008) 013004 [arXiv:0802.0007 [hep-ph]].

[50] H. L. Lai, *et al.*, Phys. Rev. D **82** (2010) 074024 [arXiv:1007.2241 [hep-ph]].

[51] L. Bourhis, M. Fontannaz and J. P. Guillet, Eur. Phys. J. C **2** (1998) 529 [arXiv:hep-ph/9704447].

[52] L. Bourhis, M. Fontannaz, J. P. Guillet and M. Werlen, Eur. Phys. J. C **19** (2001) 89 [arXiv:hep-ph/0009101].

[53] A. Gehrmann-De Ridder and E. W. N. Glover, Nucl. Phys. B **517** (1998) 269 [arXiv:hep-ph/9707224].

[54] S. Frixione, Phys. Lett. B **429**, 369 (1998) [arXiv:hep-ph/9801442].

[55] F. Arleo, K. J. Eskola, H. Paukkunen, C. A. Salgado, JHEP **1104** (2011) 055. [arXiv:1103.1471 [hep-ph]].

[56] M. Cacciari, M. Greco and P. Nason, JHEP **9805** (1998) 007 [arXiv:hep-ph/9803400];
M. Cacciari, S. Frixione and P. Nason, JHEP **0103** (2001) 006 [arXiv:hep-ph/0102134].

[57] P. Nason, S. Dawson and R. K. Ellis, Nucl. Phys. B **303** (1988) 607;
P. Nason, S. Dawson and R. K. Ellis, Nucl. Phys. B **327** (1989) 49 [Erratum-ibid. B **335** (1990) 260].

[58] M. Cacciari, P. Nason and R. Vogt, Phys. Rev. Lett. **95** (2005) 122001 [arXiv:hep-ph/0502203].

[59] N. Brambilla *et al.*, arXiv:hep-ph/0412158.

[60] R. Vogt [Hard Probe Collaboration], Int. J. Mod. Phys. E **12** (2003) 211 [arXiv:hep-ph/0111271].

[61] R. Vogt, Phys. Rev. C **71** (2005) 054902 [arXiv:hep-ph/0411378].

[62] R. Vogt, Phys. Rev. **C81** (2010) 044903. [arXiv:1003.3497 [hep-ph]].

[63] L. V. Gribov, E. M. Levin and M. G. Ryskin, Phys. Rept. **100** (1983) 1.

[64] F. Gelis, E. Iancu, J. Jalilian-Marian, R. Venugopalan, [arXiv:1002.0333 [hep-ph]].

[65] E. A. Kuraev, L. N. Lipatov and V. S. Fadin, Sov. Phys. JETP **45**, 199 (1977) [Zh. Eksp. Teor. Fiz. **72**, 377 (1977)].

[66] I. I. Balitsky and L. N. Lipatov, Sov. J. Nucl. Phys. **28**, 822 (1978) [Yad. Fiz. **28**, 1597 (1978)].

[67] K. Aamodt *et al.* [ALICE Collaboration], Phys. Rev. Lett. **106** (2011) 032301 [arXiv:1012.1657 [nucl-ex]].

[68] P. Quiroga-Arias, J. G. Milhano, U. A. Wiedemann, Phys. Rev. **C82** (2010) 034903. [arXiv:1002.2537 [hep-ph]].

[69] J. L. Albacete, C. Marquet, Phys. Lett. **B687** (2010) 174-179. [arXiv:1001.1378 [hep-ph]].

[70] E. Braidot [STAR Collaboration], Nucl. Phys. **A854** (2011) 168-174. [arXiv:1008.3989 [nucl-ex]].

[71] J. L. Albacete, C. Marquet, Phys. Rev. Lett. **105** (2010) 162301. [arXiv:1005.4065 [hep-ph]].

[72] M. Strikman, W. Vogelsang, Phys. Rev. **D83** (2011) 034029. [arXiv:1009.6123 [hep-ph]].

[73] J. L. Albacete, A. Dumitru, [arXiv:1011.5161 [hep-ph]].

[74] [CMS and TOTEM Collaborations] M. Albrow *et al.*, "Prospects for Diffractive and Forward Physics at the LHC", CERN/LHCC 2006-039/G-124

[75] C. Royon, PoS **DIS2010** (2010) 088. [arXiv:1008.3207 [hep-ex]].

[76] M. G. Albrow *et al.* [FP420 R and D Collaboration], JINST **4** (2009) T10001 [arXiv:0806.0302 [hep-ex]].

[77] Baur G, Hencken K, Trautmann D, Sadovsky S and Kharlov Y 2002, Phys. Rept. **364** 359.

[78] A. Ageev *et al.*, J. Phys. G **28** (2002) R117.

[79] C. A. Bertulani, S. R. Klein, J. Nystrand, Ann. Rev. Nucl. Part. Sci. **55** (2005) 271-310 [nucl-ex/0502005].

[80] A. J. Baltz, G. Baur, D. d'Enterria, L. Frankfurt, F. Gelis, V. Guzey, K. Hencken, (ed.), Y. .Kharlov *et al.*, Phys. Rept. **458** (2008) 1-171 [arXiv:0706.3356 [nucl-ex]].

[81] F. Carminati *et al.* [ALICE Collaboration], J. Phys. G **30** (2004) 1517.

[82] B. Alessandro *et al.* [ALICE Collaboration], J. Phys. G **32** (2006) 1295.

[83] P. Steinberg [ATLAS Collaboration], J. Phys. G **34** (2007) S527 [arXiv:0705.0382 [nucl-ex]]; S. N. White, Acta Phys. Hung. **A25** (2006) 531-537 [nucl-ex/0505020].

[84] D. d'Enterria *et al.* [CMS Collaboration], J. Phys. G **34** (2007) 2307.

[85] R. Vogt, arXiv:hep-ph/0407298.

[86] S. R. Klein, J. Nystrand and R. Vogt, Phys. Rev. C **66** (2002) 044906.

[87] M. Strikman, R. Vogt and S. White, Phys. Rev. Lett. **96** (2006) 082001 [arXiv:hep-ph/0508296].

[88] C. Adler *et al.* [STAR Collaboration], Phys. Rev. Lett. **89** (2002) 272302; B. I. Abelev *et al.* [STAR Collaboration], Phys. Rev. **C77** (2008) 034910. [arXiv:0712.3320 [nucl-ex]].

[89] S. Timoshenko, arXiv:nucl-ex/0501010.

[90] B. I. Abelev *et al.* [STAR Collaboration], Phys. Rev. Lett. **102** (2009) 112301. [arXiv:0812.1063 [nucl-ex]].

[91] B. I. Abelev *et al.* [STAR Collaboration], Phys. Rev. **C81** (2010) 044901. [arXiv:0912.0604 [nucl-ex]].

[92] D. d'Enterria *et al.* [PHENIX Collaboration], arXiv:nucl-ex/0601001.

[93] S. Afanasiev *et al.* [PHENIX Collaboration], Phys. Lett. B **679** (2009) 321 [arXiv:0903.2041 [nucl-ex]].

[94] S. N. White, AIP Conf. Proc. **792**, 527 (2005) [arXiv:nucl-ex/0507023].

[95] S. Klein and R. Vogt, Phys. Rev. C **68** (2003) 017902.

[96] S. S. Adler *et al* [PHENIX Collaboration], *Phys. Rev. Lett.* **96** (2006) 012304 [arXiv:nucl-ex/0507032].

[97] D. Bocian and K. Piotrzkowski, Acta Phys. Polon. B **35** (2004) 2417.

[98] K.-P. O. Diener, Ch. Schwanenberger and M. Spira, Eur. Phys. J. C **25** (2002) 405.

[99] U. Dreyer in A. Baltz *et al.*, arXiv:hep-ph/0702212; U. Dreyer, K. Hencken and D. Trautmann, J. Phys. G **36** (2009) 085003.

[100] D. d'Enterria and J. P. Lansberg, Phys. Rev. D **81**, 014004 (2010) [arXiv:0909.3047 [hep-ph]].

[101] M. Nagano and A.A. Watson, Rev. Mod. Phys. 72 (2000) 689, and refs. therein.

[102] M. Unger for The Pierre Auger Collaboration, Procs. of the 30th ICRC 2007, Mérida, México, arXiv:0706.1495

[103] S. Ostapchenko, Nucl. Phys. Proc. Suppl. **151** (2006) 143.

[104] R.S. Fletcher *et al.*, Phys. Rev. D **63** (2001) 054030.

[105] K. Werner *et al.*, Phys. Rev. C **74** (2006) 044902.

[106] D. d'Enterria, R. Engel, T. Pierog, S. Ostapchenko and K. Werner, arXiv:1101.5596 [astro-ph.HE].

[107] O. A. Grachov *et al.*, AIP Conf. Proc. **867** (2006) 258; S. White, Nucl. Instrum. Meth. A **617** (2010) 126; C. Oppedisano *et al.*, Nucl. Phys. Proc. Suppl. **197** (2009) 206.

[108] Technical Design Report of the LHCf experiment, CERN-LHCC-2006-004 (2006).

[109] V. Guzey, M. Strikman and W. Vogelsang, Phys. Lett. B **603**, 173 (2004) [arXiv:hep-ph/0407201].

[110] F. Arleo, D. d'Enterria and A. S. Yoon, JHEP **1006**, 035 (2010) [arXiv:1003.2963 [hep-ph]].